Available online at www.sciencedirect.com
SCIENCE DIRECT®
Journal of Molecular Catalysis A: Chemical 231 (2005) 221–233
JOURNAL OF MOLECULAR CATALYSIS A: CHEMICAL
www.elsevier.com/locate/molcata

Preparation and characterization of acylhydrazone nickel(II) complexes and their catalytic behavior in vinyl polymerization of norbornene and oligomerization of ethylene

Junxian Hou [a], Wen-Hua Sun [a,*], Dongheng Zhang [a], Liyi Chen [a], Wei Li [b], Dongfeng Zhao [b], Haibin Song [c]

[a] *Key Laboratory of Engineering Plastics, Institute of Chemistry, Chinese Academy of Sciences, Beijing 100080, China*
[b] *R&D Center, Xiangyang Chemical Corporation, Yingkou, Liaoning 115005, China*
[c] *State Key Laboratory of Functional Polymer, Nankai University, Tianjin 300071, China*

Received 12 September 2004; received in revised form 5 January 2005; accepted 6 January 2005

Abstract

The derivatives of 4,5-diazafluorene-9-one-benzoylhydrazone (**1**–**4**) and 2-pyridine-carboxaldehyde-benzoylhydrazone (**5**–**9**) were prepared. The compounds **1**–**4** reacted with $Ni(Ac)_2{\cdot}4H_2O$ to form diaquabis[4,5-diazafluorene-9-one-benzoylhydrazone]nickel(II) (**10**–**13**), while the compounds **5**–**9** reacted with $(DME)NiBr_2$ to form bis[*N*-(pyridine-2-carboxaldehyde-benzoylhydrazone)]nickel(II) dibromide (**14**–**18**), respectively. All ligands and complexes were characterized by elemental analysis and spectroscopic analysis, along with the X-ray single crystal diffraction techniques for **10**, **13** and **14**. The nickel(II) centers are six-coordinated with two corresponding ligands and two coordinated solvents for **10**–**13**, while the geometry around the nickel atom of **14**–**18** is distorted octahedron with two ligands and two bromides. Activated with methylaluminoxane, all nickel complexes show good activities for vinyl polymerization of norbornene and considerable activities for ethylene oligomerization at ambient pressure. By using **10**, the influence of reaction conditions was carefully examined on the catalytic behavior of vinyl polymerization of norbornene. The catalytic conditions were varied to investigate their effects on activity of ethylene oligomerization. The resulting poly(norbornene)s were characterized by IR, ^{1}H NMR, TGA, DSC and the viscosity measurement.

Keywords: Nickel complex; Acylhydrazone; Polynorbornene; Ethylene oligomerization

1. Introduction

The polynorbornenes have been recognized as the advanced materials with interesting and unique properties [1]. Though vinyl polymerization of norbornene was found with $TiCl_4$-based Ziegler catalyst [2], nickel-based complexes have been of more interest because of their good activity and property of resulting polynorbornene (PNB) [3–8]. The ethylene oligomerization presents one of the major industrial processes for the production of linear α-olefins, and the commercially practiced shell high olefin process (SHOP) based on nickel complex bearing P–O bidentate ligands produces olefins at 1 million tons every year [9]. Recently, various late transition metal complexes have been explored for ethylene activations [10]. In our laboratory, we have engaged in ethylene activation with various nickel complexes having chelating ligands of diimine [*N*,*N*] [11], salicylaldimine [*N*,*O*] [12] and 8-(diphenylphosphino)quinoline [*P*,*N*] [13]. Subsequently, the nickel complexes containing 8-(diphenylphosphino)quinoline [14] and salicylideneimide [15] were found to show high catalytic activity in vinyl polymerization of norbornene, and the resulting PNBs have good solubility in halogenated aromatic hydrocarbons. This has triggered a renewed interest in the development of a family of nickel complexes which are useful for both vinyl

* Corresponding author. Tel.: +86 1062557955; fax: +86 1062618239.
E-mail address: whsun@iccas.ac.cn (W.-H. Sun).

1381-1169/$ – see front matter © 2005 Elsevier B.V. All rights reserved.
doi:10.1016/j.molcata.2005.01.009

polymerization of norbornene and ethylene oligomerization. The nickel complexes containing 4,5-diazafluorene-9-one-benzoylhydrazone derivatives showed reasonable activities for ethylene oligomerization [16]. The acylhydrazone can be of two types of ketone and enolate in their nickel complexes under different condition of the complexation. The variations of these complexes are investigated here. All nickel complexes were characterized by elemental analysis and spectra measurements as well as X-ray diffraction for the molecular structures of representative complexes. In the presence of cocatalyst methylaluminoxane (MAO), all nickel complexes show reasonable catalytic activity for ethylene oligomerization and good catalytic activity for vinyl polymerization of norbornene. The influence of reaction conditions on the catalytic behavior was examined. The resulting PNBs were characterized by IR, ^{1}H NMR, TGA, DSC and the viscosity measurement.

2. Experimental

2.1. General procedures

All manipulations of air- or moisture-sensitive compounds were carried out under an atmosphere of nitrogen using standard Schlenk techniques. Toluene was refluxed over sodium-benzophenone until purple color appeared and distilled under nitrogen atmosphere prior to use. CH_2Cl_2 was dried over calcium hydride and distilled under nitrogen. Methylaluminoxane (MAO) was purchased from Albemarle as 1.4 M toluene solution. Norbornene (from Acros) was purified by distillation over potassium and used as a solution in dichloromethane or toluene. All other chemical reagents were commercially obtained unless otherwise stated.

IR spectra were recorded on a Perkin Elmer system 2000 FT-IR spectrometer. The chemical shifts of NMR spectra were measured with a Bruker BMX-300 MHz instrument and expressed in ppm using TMS as internal standard. Elemental analyses were performed by using an HP-MOD 1106 microanalyzer. Viscosity measurements were carried out in chlorobenzene at 25 °C using an Ubbelohde viscometer. Distribution of oligomers obtained was measured on a Varian Vista 6000 GC spectrometer and an HP 5971A GC–MS detector.

3. Synthesis of Schiff-base ligands and complexes

3.1. Synthesis of ligands *1*–*9*

4,5-Diazafluorene-9-one (dafo) was prepared according to the literature method [16,17]. The condensation reaction of dafo with benzoylhydrazine in ethanol gave the ligands **1**–**4** in approximately 80–95% yield. Ligands **5**–**9** were synthesized as described in the literature [18] (Scheme 1).

3.1.1. 4,5-Diazafluorene-9-one-benzoylhydrazone (*1*)

The synthesis of 4,5-diazafluorene-9-one-benzoylhydrazone (**1**) was reported in our previous paper [16]; mp: 162–164 °C. ^{1}H NMR (300 MHz, CD_3SOCD_3), δ (ppm): 7.50–7.69 (m, 5H), 8.03 (d, J = 6 Hz, 2H), 8.245 (d, J = 9 Hz, 1H), 8.545 (d, J = 9 Hz, 1H), 8.74–8.77 (t, 2H), 12.07 (NH). ^{13}C NMR (75 MHz, CD_3SOCD_3), δ (ppm): 124.3, 124.9, 125.3, 128.7, 129.1, 130.0, 132.5, 132.7, 133.3, 135.7, 152.1, 157.7, 159.0. IR (KBr, cm^{-1}): 3386 (br), 3150 (br), 3061 (w), 2927 (w), 1741 (w), 1692 (s), 1593 (m), 1564 (s), 1515 (s), 1486 (m), 1402 (s), 1341 (w), 1265 (s), 1182 (m), 1164 (m), 1132 (s), 1094 (m), 1073 (m), 1028 (w), 1001 (w). Anal. Calcd. (%) for $C_{18}H_{12}N_4O{\cdot}CH_3CH_2OH$: C, 69.35; H, 5.24; N 16.17. Found (%): C, 69.24; H, 5.16; N, 16.49.

3.1.2. 4,5-Diazafluorene-9-one-2-methylbenzoylhydrazone (*2*)

4,5-Diazafluorene-9-one (360 mg, 2 mmol) was added to a solution of 2-methylbenzoylhydrazine (280 mg, 2 mmol) in absolute ethanol (30 ml). After the addition of *p*-toluene sulfonic acid (catalytic amount), the solution was refluxed for 6 h. The ethanol was partly removed in vacuum and the remainder was kept cool over night. Yellow crystalline product, **2**, was obtained, which was then washed with ethanol and dried in a vacuum oven overnight. Yield 540 mg (80%); mp: 221–223 °C. ^{1}H NMR (300 MHz, CD_3SOCD_3), δ (ppm): 2.55 (s, 3H), 7.29–7.37 (m, 4H), 7.42–7.50 (m, 1H), 7.55–7.58 (d, J = 7 Hz, 1H), 8.20 (s, 2H), 8.74 (d, J = 3 Hz, 1H), 8.81 (d, J = 5 Hz, 1H), 9.90 (NH) ppm. ^{13}C NMR (75 MHz, CD_3SOCD_3), δ (ppm): 39.8, 123.9, 124.7, 124.9, 126.0, 128.1, 129.6, 130.6, 131.0, 132.6, 134.9, 135.2, 136.5, 151.9, 157.4, 158.9. IR (KBr, cm^{-1}): 3339 (w), 3272 (w), 3092 (w), 3060 (w), 2962 (w), 2928 (w), 2856 (w), 1674 (s), 1607 (m), 1589 (m), 1562 (m), 1488 (m), 1456 (m), 1402 (s), 1343 (s), 1284 (m), 1205 (w), 1179 (w), 1165 (w), 1142 (m), 1112 (w), 1085 (m), 1045 (w). Anal. Calcd. (%) for $C_{19}H_{14}N_4O{\cdot}(1/2)$EtOH: C, 71.20; H, 5.08; N, 16.61. Found (%): C, 71.64; H, 5.06; N, 16.51.

3.1.3. 4,5-Diazafluorene-9-one-3-methylbenzoylhydrazone (*3*)

Compound **3** was synthesized by a procedure similar to that for **2** except that 3-methylbenzoylhydrazine was used, and was obtained as yellow powder. Yield 590 mg (87%); mp: 160–162 °C. ^{1}H NMR (300 MHz, CD_3SOCD_3), δ (ppm): 2.48 (s, 3H), 7.27–7.46 (m, 4H), 7.75 (s, 1H), 7.82 (s, 1H), 8.20 (t, J = 9 Hz, 2H), 8.75 (d, J = 5 Hz, 1H), 8.81 (d, J = 5 Hz, 1H), 10.03 (NH). ^{13}C NMR (75 MHz, CD_3SOCD_3), δ (ppm): 39.9, 124.4, 124.9, 125.4, 125.8, 129.0, 129.1, 130.0, 132.6, 133.2, 133.3, 135.7, 138.5, 152.1, 157.7, 159.0. IR (KBr, cm^{-1}): 3203 (br), 3062 (w), 3012 (w), 2965 (w), 2922 (w), 1734 (w), 1696 (s), 1672 (s), 1588 (m), 1564 (m), 1512 (s), 1401 (s), 1340 (w), 1274 (s), 1196 (s), 1128 (m), 1096 (m), 1050 (w), 1001 (w). Anal. Calcd. (%) for $C_{19}H_{14}N_4O{\cdot}(1/2)$EtOH: C, 71.20; H, 5.08; N, 16.61. Found (%): C, 70.88; H, 5.00; N, 16.47.

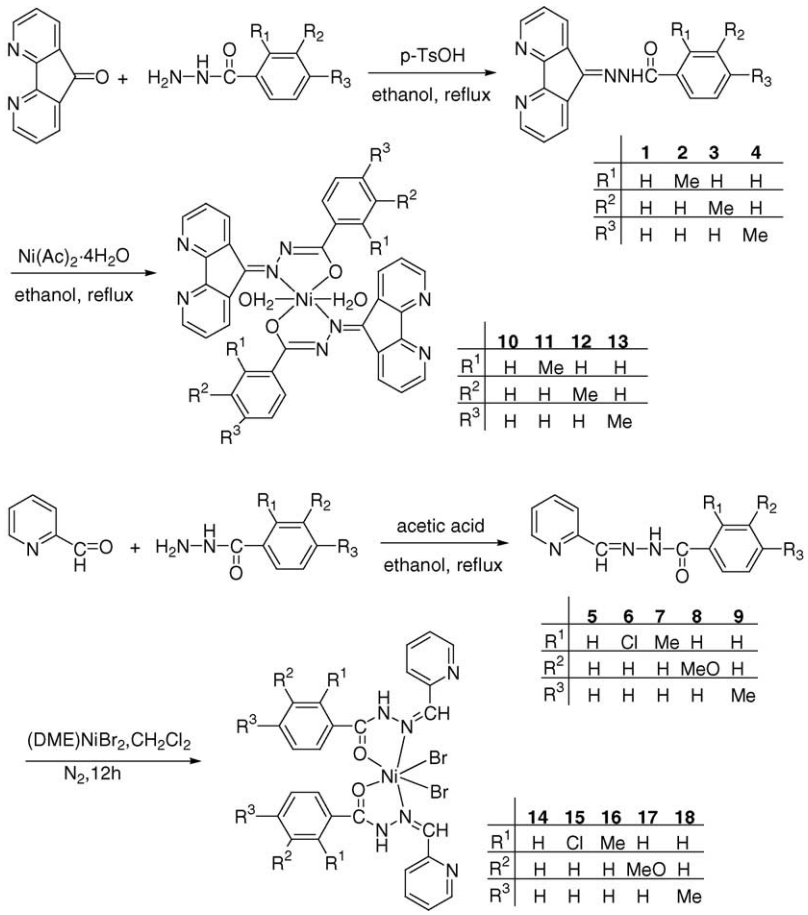

Scheme 1. Synthesis of ligands **1**–**9** and their complexes **10**–**18**.

*3.1.4. 4,5-Diazafluorene-9-one-4-methylbenzoylhydrazone (**4**)*

Compound **4** was prepared with 4-methylbenzoylhydrazine according to the above synthetic procedure, and was obtained as yellow powder. Yield 610 mg (95%); mp: 282–284 °C. ^{1}H NMR (300 MHz, CD_3SOCD_3), δ (ppm): 2.48 (s, 3H), 7.29–7.44 (m, 4H), 7.89–7.91 (d, J = 8 Hz, 2H), 8.21 (t, J = 7 Hz, 2H), 8.75 (d, J = 5 Hz, 1H), 8.81 (d, J = 5 Hz, 1H), 10.00 (NH). ^{13}C NMR (75 MHz, CD_3SOCD_3), δ (ppm): 39.9, 124.4, 124.9, 125.4, 128.8, 129.7, 130.0, 130.4, 132.6, 135.7, 143.0, 152.2, 157.8, 159.1. IR (KBr, cm^{-1}): 3366 (br), 3231 (br), 3079 (w), 3011 (w), 2918 (w), 1697 (s), 1608 (m), 1584 (w), 1564 (m), 1527 (s), 1501 (s), 1471 (w), 1400 (s), 1339 (w), 1289 (w), 1259 (s), 1185 (m), 1163 (m), 1135 (m), 1118 (w), 1090 (m), 1039 (w), 1018 (w). Anal. Calcd. (%) for $C_{19}H_{14}N_4O\cdot(1/3)H_2O$: C, 71.24; H, 4.61; N, 17.49. Found (%): C, 71.53; H, 4.57; N, 17.34.

*3.1.5. 2-Pyridinecarboxaldehyde-benzoylhydrazone (**5**)*

The ethanol solution containing the aldehyde (540 mg, 0.5 mmol) with a stoichiometric amount of the corresponding hydrazide was refluxed in the presence of a few drops of glacial acetic acid. TLC was used to monitor the reaction with the disappearance of the corresponding stain to the reactants (12 h). After concentrating and cooling the solution, the product, **5**, was crystallized as colorless needles, and then washed with a few milliliters of diethyl ether and dried in vacuum. Yield: 870 mg (73%). The ligand was previously reported [18] and its structures are confirmed with ^{1}H NMR and IR. IR (KBr, cm^{-1}): 3445 (br), 3034 (m), 1684 (s), 1596 (m), 1532 (s), 1481 (m), 1423 (m), 1301 (m), 1268 (s), 1185 (w), 1136 (m), 1103 (m), 1077 (w), 1051 (m).

*3.1.6. 2-Pyridinecarboxaldehyde-2-chlorobenzoylhydrazone (**6**)*

Compound **6** was prepared according to the synthetic procedure for **5** except that 2-chlorobenzoylhydrazine was used instead of benzoylhydrazine, and was obtained as colorless crystals. Yield 1030 mg (75%); mp: 112–114 °C. ^{1}H NMR (300 MHz, CD_3SOCD_3), δ (ppm): 7.39–7.59 (m, 5H), 7.69–7.76 (m, 2H), 8.03–8.05 (d, J = 7 Hz, 1H), 8.80 (s, 1H), 15.00 (NH). ^{13}C NMR (75 MHz, CD_3SOCD_3), δ (ppm): 124.9, 127.0, 127.8, 128.8, 130.8, 132.3, 136.7, 138.6, 139.7, 148.2, 151.6, 162.7, 169.5. IR (KBr, cm^{-1}): 3442 (br), 3058 (m), 1667 (s), 1599 (m), 1559 (w), 1477 (m), 1455 (m), 1416

(s), 1337 (s), 1298 (m), 1264 (w), 1246 (m), 1148 (m), 1110 (m), 1048 (m), 1030 (w), 1002 (m). Anal. Calcd. (%) for $C_{13}H_{10}N_3OCl$: C, 60.12; H, 3.88; N, 16.18; Cl, 13.65. Found (%): C, 60.25; H, 3.92; N, 16.20; Cl, 13.70.

3.1.7. 2-Pyridinecarboxaldehyde-2-methylbenzoylhydrazone (7)

Compound **7** was prepared with 2-methylbenzoylhydrazine instead of benzoylhydrazine in the synthesis of **5**, and was obtained as colorless crystals. Yield 900 mg (71%); mp: 106–108 °C. ^{1}H NMR (300 MHz, $CDCl_3$), δ (ppm): 2.57 (s, 3H), 7.13–7.59 (m, 7H), 7.86 (s, 1H), 8.55 (s, 1H), 14.92 (NH). ^{13}C NMR (75 MHz, $CDCl_3$), δ (ppm): 20.3, 124.1, 125.9, 127.6, 130.6, 131.4, 134.4, 135.6, 137.9, 138.4, 148.1, 152.3, 167.0. IR (KBr, cm^{-1}): 3433 (br), 3341 (w), 3148 (m), 3052 (m), 2972 (m), 2927 (m), 2854 (w), 1679 (s), 1601 (m), 1501 (s), 1481 (s), 1429 (m), 1378 (w), 1296 (m), 1265 (m), 1248 (m), 1208 (w), 1165 (w), 1141 (m), 1103 (s), 1047 (s), 1012 (w). Anal. Calcd. (%) for $C_{14}H_{13}N_3O$: C, 70.28; H, 5.48; N, 17.56. Found (%): C, 70.07; H, 5.49; N, 17.53.

3.1.8. 2-Pyridinecarboxaldehyde-3-methoxybenzoylhydrazone (8)

Similarly, **8** was prepared with 3-methoxybenzoylhydrazine and obtained as colorless crystals. Yield 1040 mg (77%); mp: 100–102 °C. ^{1}H NMR (300 MHz, $CDCl_3$), δ (ppm): 3.85 (s, 3H), 7.08 (d, J = 8 Hz, 1H), 7.37–7.44 (m, 2H), 7.52 (d, J = 8 Hz, 4H), 7.90 (t, J = 8 Hz, 1H), 8.70 (d, J = 4 Hz, 1H), 15.51 (NH). ^{13}C NMR (75 MHz, $CDCl_3$), δ (ppm): 54.0, 111.4, 117.0, 118.1, 123.0, 124.8, 128.5, 133.0, 136.8, 137.4, 146.7, 150.8, 158.5, 162.8. IR (KBr, cm^{-1}): 3434 (br), 3067 (w), 3005 (w), 2970 (w), 2939 (w), 2836 (w), 1682 (s), 1596 (m), 1534 (m), 1473 (m), 1427 (w), 1381 (w), 1328 (w), 1293 (s), 1276 (s), 1238 (s), 1181 (w), 1159 (w), 1106 (w), 1080 (w), 1048 (w). Anal. Calcd. (%) for $C_{14}H_{13}N_3O_2$: C, 65.87; H, 5.13; N, 16.46. Found (%): C, 65.59; H, 5.15; N, 16.42.

3.1.9. 2-Pyridinecarboxaldehyde-4-methylbenzoylhydrazone (9)

The compound **9** was prepared with 4-methylbenzoylhydrazine and formed as colorless crystals. Yield 990 mg (78%); mp: 139–141 °C. ^{1}H NMR (300 MHz, $CDCl_3$), δ (ppm): 2.40 (s, 3H), 7.30–7.38 (m, 3H), 7.50 (d, J = 9 Hz, 2H), 7.89 (s, 3H), 8.71 (s, 1H), 15.47 (NH). ^{13}C NMR (75 MHz, $CDCl_3$), δ (ppm): 21.4, 124.0, 125.8, 127.4, 129.3, 130.0, 137.9, 138.2, 142.6, 147.9, 152.0, 164.2. IR (KBr, cm^{-1}): 3437 (br), 3053 (w), 3029 (w), 2997 (w), 1667 (s), 1612 (m), 1593 (m), 1559 (w), 1535 (m), 1502 (m), 1478 (m), 1427 (m), 1400 (w), 1316 (w), 1296 (m), 1273 (s), 1251 (m), 1190 (w), 1156 (w), 1118 (m), 1105 (m), 1049 (s), 1006 (w). Anal. Calcd. (%) for $C_{14}H_{13}N_3O$: C, 70.28; H, 5.48; N, 17.56. Found (%): C, 70.51; H, 5.62; N, 17.85.

3.2. Synthesis of complexes

3.2.1. 4,5-Diazafluorene-9-one-benzoylhydrazone nickel(II) complex (10) [19]

4,5-Diazafluorene-9-one-benzoylhydrazone (69 mg, 0.2 mmol) (**1**) was dissolved in ethanol (20 ml). Into this solution, an ethanol solution (5 ml) of $Ni(Ac)_2{\cdot}4H_2O$ (25 mg, 0.1 mmol) was added dropwise. The mixture was refluxed for 24 h and yellow precipitate resulted. The product was filtered, washed with hot ethanol and dried in a vacuum oven. Yield 54 mg (73%); mp: >320 °C. Red crystals of **10** suitable for X-ray measurement were obtained by slow evaporation of a solution of **10** in its DMF solution. IR (KBr, cm^{-1}): 3399 (br), 3063 (w), 2925 (w), 1589 (m), 1564 (m), 1501 (s), 1484 (s), 1436 (m), 1406 (m), 1366 (s), 1350 (s), 1297 (m), 1171 (m), 1147 (w), 1091 (w), 1044 (s), 1003 (w).

3.2.2. 4,5-Diazafluorene-9-one-2-methylbenzoylhydrazone nickel(II) complex (11)

In a similar procedure as described for **10**, complex **11** was synthesized in the reaction of $Ni(Ac)_2{\cdot}4H_2O$ and **2** as a yellow powder. Yield 56 mg (77%); mp: >320 °C. IR (KBr, cm^{-1}): 3393 (br), 3064 (w), 2961 (w), 2925 (w), 1579 (m), 1563 (m), 1496 (s), 1426 (m), 1407 (s), 1345 (s), 1274 (m), 1163 (m), 1111 (m), 1088 (m), 1042 (s). Anal. Calcd. (%) for $C_{38}H_{26}N_8O_2Ni{\cdot}2H_2O$: C, 63.27; H, 4.19; N, 15.53. Found (%): C, 62.92; H, 3.93; N, 15.32.

3.2.3. 4,5-Diazafluorene-9-one-3-methylbenzoylhydrazone nickel(II) complex (12)

In a similar manner as described for **10**, the complex **12** was prepared by the reaction of $Ni(Ac)_2{\cdot}4H_2O$ and **3** as a yellow powder. Yield 59 mg (79%); mp: >320 °C. IR (KBr, cm^{-1}): 3396 (br), 3064 (w), 2923 (w), 1589 (m), 1563 (m), 1501 (s), 1470 (s), 1407 (s), 1347 (s), 1281 (m), 1217 (m), 1164 (w), 1135 (w), 1087 (w), 1045 (s). Anal. Calcd. (%) for $C_{38}H_{26}N_8O_2Ni{\cdot}2H_2O$: C, 63.27; H, 4.19; N, 15.53. Found (%): C, 63.00; H, 4.11; N, 15.44.

3.2.4. 4,5-Diazafluorene-9-one-4-methylbenzoylhydrazone nickel(II) complex (13)

In a similar manner as described for **10**, complex **13** was prepared by reacting $Ni(Ac)_2{\cdot}4H_2O$ with **4** as a yellow powder. Yield 59 mg (80%); mp: >320 °C. Dark red crystals of **13** suitable for X-ray measurement were obtained by slow evaporation of its DMF solution. IR (KBr, cm^{-1}): 3395 (br), 3064 (w), 2923 (w), 1611 (w), 1583 (m), 1514 (m), 1482 (s), 1428 (w), 1406 (s), 1348 (s), 1296 (m), 1177 (m), 1147 (w), 1090 (w), 1044 (s). Anal. Calcd. (%) for $C_{38}H_{26}N_8O_2Ni{\cdot}2H_2O$: C, 63.27; H, 4.19; N, 15.53. Found (%): C, 63.84; H, 4.19; N, 15.30.

*3.2.5. Bis[N-(pyridine-2-carboxaldehyde)benzoylhydrazone]nickel(II) dibromide (**14**)*

N-(Pyridine-2-carboxaldehyde)benzoylhydrazone (**5**) (90 mg, 0.4 mmol) was dissolved in dichloromethane (15 ml). A dichloromethane solution (5 ml) of (DME)$NiBr_2$ (62 mg, 0.2 mmol) was added dropwise. The mixture was stirred at room temperature for 12 h and the nickel complex was precipitated as a yellow-green powder. The product was filtered, washed with dichloromethane and dried in a vacuum oven. Yield 115 mg (86%); mp: 189–191 °C. Yellow-green crystals of **14** suitable for single-crystal X-ray measurement were obtained by slow diffusion of ethyl ether into its dichloromethane solution. IR (KBr, cm^{-1}): 3402 (br), 3061 (w), 3006 (w), 1630 (s), 1574 (s), 1520 (s), 1480 (s), 1428 (m), 1306 (m), 1290 (m), 1104 (m), 1062 (m), 1003 (m). Anal. Calcd. (%) for $C_{26}H_{22}N_6O_2NiBr_2$: C, 46.68; H, 3.31; N, 12.56. Found (%): C, 46.37; H, 3.40; N, 12.37.

*3.2.6. Bis[N-(pyridine-2-carboxaldehyde)-2-chlorobenzoylhydrazone]nickel(II) dibromide (**15**)*

In a similar manner as described for **14**, the nickel complex **15** was obtained as a yellow-green powder in the reaction of (DME)$NiBr_2$ and **6**. Yield 125 mg (85%); mp: 254–256 °C. IR (KBr, cm^{-1}): 3429 (br), 3039 (w), 3001 (w), 1601 (s), 1559 (w), 1492 (s), 1463 (s), 1418 (m), 1304 (m), 1259 (w), 1128 (w), 1102 (w), 1062 (s), 1002 (w). Anal. Calcd. (%) for $C_{26}H_{20}N_6O_2NiBr_2Cl_2{\cdot}H_2O$: C, 41.31; H, 2.93; N, 11.12. Found (%): C, 41.34; H, 2.72; N, 11.07.

*3.2.7. Bis[N-(pyridine-2-carboxaldehyde)-2-methylbenzoylhydrazone]nickel(II) dibromide (**16**)*

In a similar manner as described for **14**, the nickel complex **16** was formed as a yellow-green powder from the reaction of (DME)$NiBr_2$ and **7**. Yield 106 mg (76%); mp: 172–174 °C. IR (KBr, cm^{-1}): 3430 (br), 3055 (w), 2957 (w), 1616 (s), 1597 (m), 1568 (m), 1510 (s), 1477 (s), 1427 (m), 1302 (m), 1255 (w), 1155 (w), 1109 (m), 1064 (m), 1002 (w). Anal. Calcd. (%) for $C_{28}H_{26}N_6O_2NiBr_2{\cdot}H_2O$: C, 47.03; H, 3.95; N, 11.75. Found (%): C, 46.89; H, 3.79; N, 11.44.

*3.2.8. Bis[N-(pyridine-2-carboxaldehyde)-3-methoxybenzoylhydrazone]nickel(II) dibromide (**17**)*

In a similar manner as described for **14**, the complex **17** was prepared by the reaction of (DME)$NiBr_2$ and ligand **8**, as a yellow-green powder. Yield 128 mg (88%); mp: 202–204 °C. IR (KBr, cm^{-1}): 3417 (br), 3049 (w), 2965 (w), 1620 (s), 1599 (m), 1579 (s), 1520 (s), 1483 (s), 1434 (m), 1312 (s), 1257 (m), 1240 (m), 1160 (w), 1129 (m), 1070 (m), 1031 (w), 1005 (w). Anal. Calcd. (%) for $C_{28}H_{26}N_6O_4NiBr_2{\cdot}H_2O$: C, 45.02; H, 3.78; N, 11.25. Found (%): C, 44.82; H, 3.53; N, 11.02.

*3.2.9. Bis[N-(pyridine-2-carboxaldehyde)-4-methylbenzoylhydrazone]nickel(II) dibromide (**18**)*

In a similar manner as described for **14**, the complex **18** was prepared by the reaction of (DME)$NiBr_2$ and **9**, as a yellow-green powder. Yield 114 mg (82%); mp: 220–222 °C. IR (KBr, cm^{-1}): 3404 (br), 3041 (w), 3003 (w), 2971 (w), 1624 (s), 1567 (m), 1532 (s), 1495 (s), 1428 (m), 1303 (s), 1254 (m), 1218 (w), 1189 (m), 1146 (w), 1122 (m), 1102 (m), 1066 (s), 1002 (w). Anal. Calcd. (%) for $C_{28}H_{26}N_6O_2NiBr_2{\cdot}0.5H_2O$: C, 47.63; H, 3.85; N, 11.90. Found (%): C, 47.46; H, 3.76; N, 11.76.

3.3. Polymerization of norbornene

In a typical procedure, the complex **10** (8 μmol) was dissolved in a Schlenk tube in 19.01 ml degassed CH_2Cl_2 under nitrogen and a 5.56 ml CH_2Cl_2 solution of norbornene (7.20 M, 40 mmol of norbornene) was added via a syringe. The polymerization was initiated by adding 0.43 ml toluene solution of 1.4 M MAO (0.60 mmol). After 30 min, the polymerization was terminated by injecting 200 ml acidic methanol (methanol:$HCl_{conc.}$ = 95:5) into the reactor. The polynorbornene was isolated by filtration, washed with methanol, and dried in vacuum at 100 °C for 100 h. The total reaction volume of norbornene polymerization was 25 ml unless otherwise stated, that was achieved by adding solvent when necessary. Similarly, the polymerization of norbornene was also carried out by using toluene as the solvent.

3.4. Ethylene oligomerization

A flame dried three-necked round bottom flask was vacuum-filled three times with nitrogen and loaded with the complex (**10**–**18**). Charged with ethylene, the freshly distilled toluene was added and the solution was stirred for 10 min to sufficiently absorb ethylene in toluene. Then co-catalyst, MAO, was added by a syringe to initiate the ethylene oligomerization. The reaction mixture was stirred under 1 atm ethylene pressure for a desired time, and the catalytic reaction was terminated with dilute HCl solution. An aliquot of the reaction mixture was analyzed by GC and GC–MS.

3.5. X-ray crystallography measurements

Intensity data of crystal were collected on a Bruker Smart 1000 CCD diffractometer at 293(2) K with graphite monochromated Mo Kα radiation (λ = 0.71073 Å). Cell parameters were obtained by global refinement of the positions of all collected reflections. Intensities were corrected for Lorentz and polarization effects and empirical absorption. The structures were solved by direct methods and refined by full-matrix least-squares on F^2. Each H atom was placed in a calculated position and refined anisotropically. Structure solution and refinement were performed using the SHELXL-97 Package [20]. Crystal data and processing pa-

Table 1
Crystallographic data of complexes **10**, **13** and **14**

	Complex **10**	Complex **13**	Complex **14**
Empirical formula	$C_{36}H_{26}N_8NiO_4$	$C_{50}H_{54}N_{12}NiO_6$	$C_{29}H_{28}Br_2Cl_6N_6NiO_2$
Formula weight	693.36	977.76	923.80
Crystal color	Red	Red	Green
Crystal size (mm)	0.18 × 0.16 × 0.12	0.10 × 0.08 × 0.06	0.32 × 0.20 × 0.18
Crystal system	Monoclinic	Triclinic	Monoclinic
Space group	*C*2/*c*	*P*-1	*C* 2/*c*
a (Å)	17.631(7)	9.611(4)	22.913(2)
b (Å)	7.248(3)	11.085(5)	12.3282(13)
c (Å)	23.876(10)	12.297(5)	17.2771(15)
α (°)	90	100.497(6)	90
β (°)	98.320(8)	97.054(6)	130.504
γ (°)	90	109.640(7)	90
V (Å^3)	3019(2)	1189.2(8)	3710.8(6)
Z	4	1	4
D_{calc} (g cm^{-3})	1.525	1.365	1.654
μ(Mo Kα) (mm^{-1})	0.700	0.472	3.145
F(0 0 0)	1432	514	1840
Temperature (K)	293(2)	293(2)	293(2)
λ (Å)	0.71073	0.71073	0.71073
θ range (°)	2.33–25.02	1.72–26.39	3.22–26.35
Reflections collected	6035	6841	6896
Independent reflections	2672	4789	3733
R_{int}	0.0673	0.0316	0.0451
Goodness-of-fit on F2	1.011	1.111	0.998
Parameters	225	318	208
Final *R* indices ($I > 2\sigma(I)$)	$R_1 = 0.0500$, $wR_2 = 0.0838$	$R_1 = 0.0539$, $wR_2 = 0.1361$	$R_1 = 0.0518$, $wR_2 = 0.989$
R indices (all data)	$R_1 = 0.0938$, $wR_2 = 0.0948$	$R_1 = 0.0907$, $wR_2 = 0.1593$	$R_1 = 0.1138$, $wR_2 = 0.1213$

rameters are summarized in Table 1. Crystallographic data for the structural analysis has been deposited with the Cambridge Crystallographic Data Center, CCDC Nos. 258309, 258310 and 258311 for complexes **10**, **13** and **14**, respectively.

4. Results and discussion

4.1. Synthesis and spectroscopic characterization

All ligand compounds were prepared in good yields according to the modified procedure [18,19]. According to a reported method [19], an ethanol solution of $Ni(Ac)_2{\cdot}4H_2O$ was added dropwise into the ethanol solution containing ligands **1**–**4**, respectively. The corresponding nickel complexes **10**–**13** were obtained as yellow precipitate. The nickel complexes **14**–**18** were synthesized by the reaction of (DME)$NiBr_2$ (DME: ethylene glycol dimethyl ether) and corresponding ligands **5**–**9** in CH_2Cl_2. The resulting complexes were precipitated from the reaction solutions after several hours.

The weak broad bands between 3060 and 3445 cm^{-1} in the IR spectra of **1**–**9** are ascribed to the stretching vibration of N–H and O–H. Characteristic band of ν(C=O) at 1667–1697 cm^{-1} for the free ligand is an indication of the keto-form in the solid state. The bands of ν(C=O) have disappeared for the complexes **10**–**13**; however, the resultant three new strong absorptions are observed around 1500, 1480, and 1296 cm^{-1} which are due to ν(C=N–N=C), ν(N=C–O), and ν(C–O), respectively. This indicates that the ligands undergo tautomerization from the keto-form to the enol-form during complexation. In IR spectra of **14**–**18**, the strong absorption bands in the range 1601–1630 cm^{-1} are ascribed to the C=O stretching vibration, while the values are found to be in the region of 1667–1684 cm^{-1} for the free ligands **5**–**9**.

4.2. Structural features

The molecular structure of **10** is shown in Fig. 1. The selected atomic distances and bond angles are listed in Table 2. The solid structure of **10** is centrosymmetric with the nickel atom located in a distorted octahedral environment with two azomethine N and two enolic O atoms of two ligands in the equation plane and two water O donors in the opposite axial sites. The five-membered chelating ring Ni(1)–O(1)–C(12)–N(2)–N(1) is nearly planar with a mean deviation of 0.1108 Å from the least-square plane and a bite angle O(1)–Ni(1)–N(1) of 76.19(10)°. The planar phenyl ring forms a dihedral angle of 29.9° with the chelating ring. The diazafluorene moiety also shows good planarity with the mean deviation of 0.0371 Å and is inclined by 13.5 and 38.6° from the chelating ring and the phenyl ring, respectively. It is noted that the C_{amide}–N bond distance (1.308(4) Å) in **10** is shorter than the C···N distance of the diazafluorene

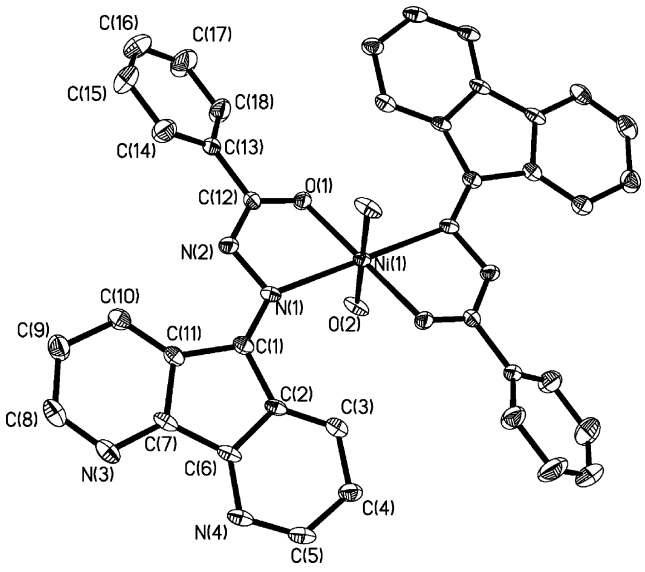

Fig. 1. Molecular structure of **10**, showing 30% probability displacement ellipsoids with hydrogen atoms omitted for clarity.

moiety (1.317(4)–1.322(5) Å), indicating its double bond nature. Compared to the relevant structural parameters of the ligand [21], the $C_{diazafluorene}$–N (1.298(4) Å) and C_{amide}–O (1.248(4) Å) bonds are elongated and C_{amide}–N bond is shortened (1.290(3), 1.216(3), 1.378(3) Å in HL·H_2O, respectively). These facts confirm that the ligand was transformed to an enol form in **10**.

The crystal packing showing intermolecular hydrogen bonds and π–π stacking interactions is depicted in Fig. 2(a). The different distances of hydrogen bonds are indicative of the different charge density of the two nitrogen atoms in the diazafluorene moiety. The water molecule H_2O(2AB) coordinated to Ni(1B) used its two hydrogens to form two hydrogen bonds with diazafluorene N(3AG) and N(4D) atoms with distances O(2AB) · · · N(3AG) and O(2AB) · · · N(4D) of 2.840 and 2.813 Å, respectively. Fig. 2(b) shows three neighboring diazafluorene moieties depicting the π–π stackings. The three diazafluorene moieties of neighboring molecules are parallel to each other, and there exist two types of π–π stackings. The diazafluorene moiety including N(3AB) has stacking with the diazafluorene moieties containing N(3E) and N(3D), respectively, and the shortest center-to-center distances are 3.292 Å (between the centers of two five-membered rings) and 3.390 Å (between the centers of five- and six-membered rings), respectively. These short separations between the rings indicate the existence of the strong intermolecular π–π stacking interaction [22]. On the whole, every molecule is linked with four of its neighboring molecules through eight intermolecule H bonds and four intermolecule π–π stacking interactions forming a two-dimensional hydrogen bond system.

Complex **13** is a centrosymmetric neutral molecule with the nickel center of symmetry, in which there are two ligands and two coordinated DMF molecules (Fig. 3). The metal atoms in the complex are hexa-coordinated by N_2O_4 in a distorted octahedral geometry with $N_{azomethine}$ and O_{amide} atoms from two enolic mononegative HL groups in the equatorial plane, forming restricted bite angles $N_{azomethine}$–M–O_{amide} of 76.77(10)°, while the O atoms from two solvent molecules occupy the axial sites. The five-membered chelating ring Ni–N–N–C–O in the equatorial plane is nearly planar with mean deviation from least-square planes of 0.1280 Å. It forms dihedral angles of 22.2° for **13** with diazafluorene ring and 11.6° with the phenyl ring. The $C_{diazafluorene}$–N, C_{amide}–O and C_{amide}–N bond distances are 1.311(4), 1.273(4) and 1.327(4) Å, respectively.

The nickel atom in the complex **14** is hexa-coordinated (Fig. 4). The dihedral angle of the two planes formed by Ni(1)–O(1)–N(2) and Ni(1)–O(1A)–N(2A) is 101.9°. The chelating ring is inclined with 11.3° from the phenyl ring and 5.3° from pyridyl ring, respectively. The two

Table 2
Selected bond lengths (Å) and angles (°) for **10**, **13** and **14**

Complex **10**		Complex **13**		Complex **14**	
Bond lengths					
Ni(1)–O(1)	1.962(2)	Ni(1)–O(1)	2.003(2)	Ni(1)–O(1)	2.109(4)
Ni(1)–N(1)	2.217(3)	Ni(1)–N(2)	2.154(3)	Ni(1)–N(2)	2.075(4)
Ni(1)–O(2)	2.045(2)	Ni(1)–O(2)	2.085(2)	Ni(1)–Br(1)	2.5061(9)
O(1)–C(12)	1.248(4)	O(1)–C(1)	1.273(4)	O(1)–C(7)	1.240(6)
N(2)–C(12)	1.308(4)	N(1)–C(1)	1.327(4)	N(1)–C(7)	1.342(6)
N(1)–N(2)	1.369(4)	N(2)–N(1)	1.392(4)	N(2)–N(1)	1.381(5)
Bond angles					
O(1)–Ni(1)–O(2A)	89.04(10)	O(1)–Ni(1)–O(2A)	90.22(10)	O(1)–Ni(1)–N(2)	77.58(15)
O(1)–Ni(1)–N(1)	76.19(10)	O(1)–Ni(1)–N(2)	76.77(10)	O(1)–C(7)–N(1)	120.9(5)
O(2)–Ni(1)–N(1)	94.80(10)	O(2)–Ni(1)–N(2)	88.79(10)	C(7)–O(1)–Ni(1)	113.2(3)
C(12)–O(1)–Ni(1)	112.3(2)	C(1)–O(1)–Ni(1)	111.0(2)	Ni(1)–N(2)–N(1)	110.8(3)
N(2)–N(1)–Ni(1)	107.30(18)	N(1)–N(2)–Ni(1)	108.72(19)	O(1)–Ni(1)–O(1A)	80.5(2)
O(1A)–Ni(1)–O(2A)	90.96(10)	O(1A)–Ni(1)–O(2A)	89.78(10)	C(7)–N(1)–N(2)	117.4(4)
O(1A)–Ni(1)–N(1)	103.81(10)	O(1A)–Ni(1)–N(2)	103.23(10)	O(1)–Ni(1)–Br(1)	91.23(10)
O(2A)–Ni(1)–N(1)	85.20(10)	O(2A)–Ni(1)–N(2)	91.21(10)	N(2)–Ni(1)–Br(1)	91.36(11)
C(12)–N(2)–N(1)	111.8(3)	C(1)–N(1)–N(2)	110.7(3)	Br(1A)–Ni(1)–Br(1)	97.83(5)
O(1)–C(12)–N(2)	127.1(3)	O(1)–C(1)–N(1)	126.1(3)	N(2)–Ni(1)–Br(1A)	95.88(11)

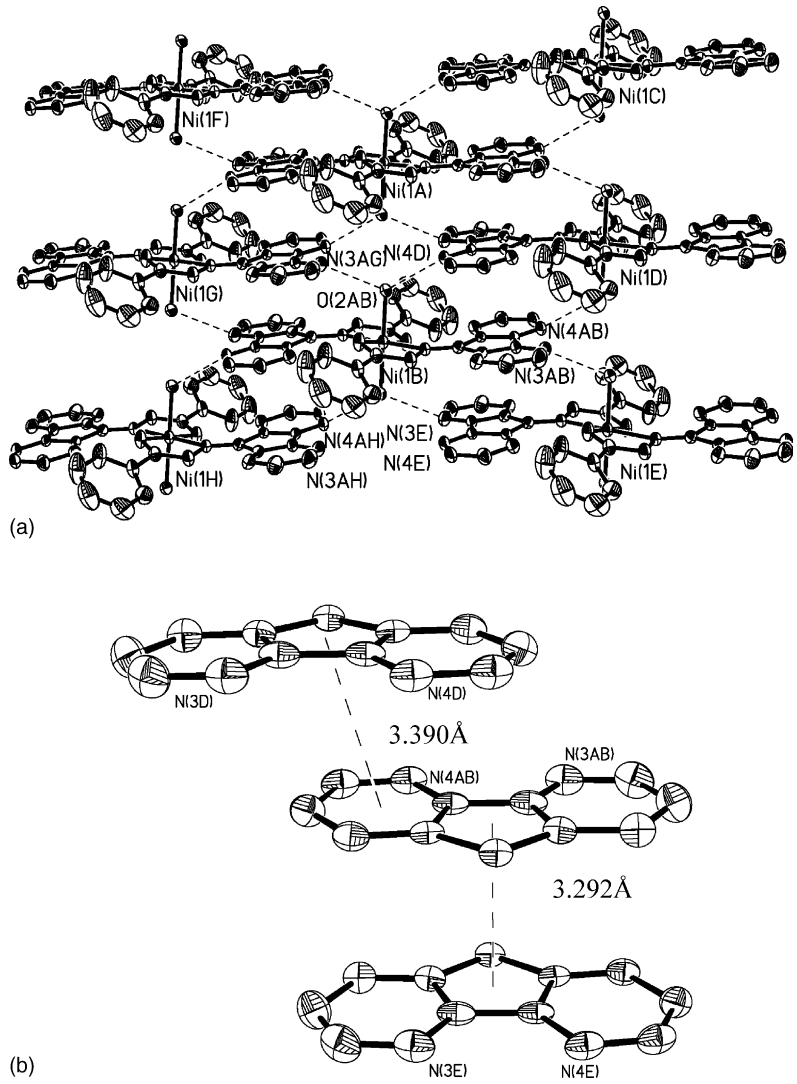

Fig. 2. (a) Crystal packing of **10** showing intermolecular hydrogen bonds and π–π stacking interactions; (b) diagram of the diazafluorene units in **10** showing the intermolecular π–π stacking.

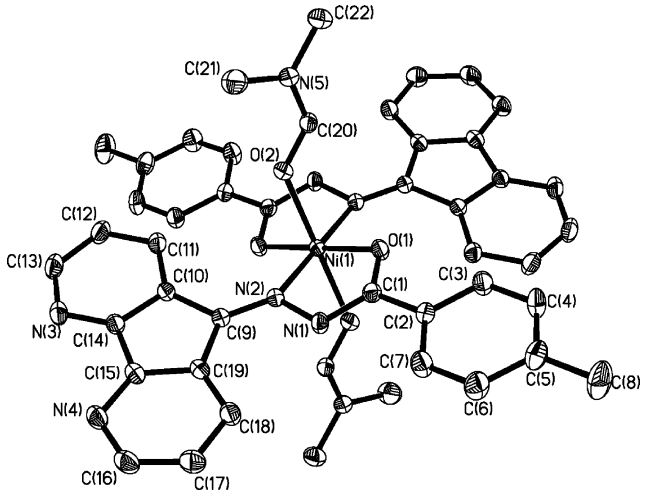

Fig. 3. Molecular structure of **13**, showing 30% probability displacement ellipsoids with hydrogen atoms and molecules of DMF omitted for clarity.

bromine atoms occupy *cis*-positions. The bond lengths of Ni(1)–Br(1), Ni(1)–O(1), Ni(1)–N(2) and C(7)–O(1) are 2.5061(9), 2.109(4), 2.075(4) and 1.240(6) Å, respectively. These facts confirm that the ligand in **14** is not in the enol form. The N(3) atom in the pyridyl ring is not coordinated to the metal center, forming intra-molecular hydrogen bond with the hydrogen in the N(1) atom.

4.3. Polymerization of norbornene

Complexes **10**–**18** exhibited remarkable catalytic activities for polymerization of norbornene in the presence of MAO. The catalytic activities of norbornene polymerization of the vinyl addition type have been affected by several parameters, including the nature of catalytic precursors, reaction temperature, monomer concentration [23,15] and reaction time as well as the viscosity of resulting polynorbornene (Table 3). The polymer yields were slightly low for

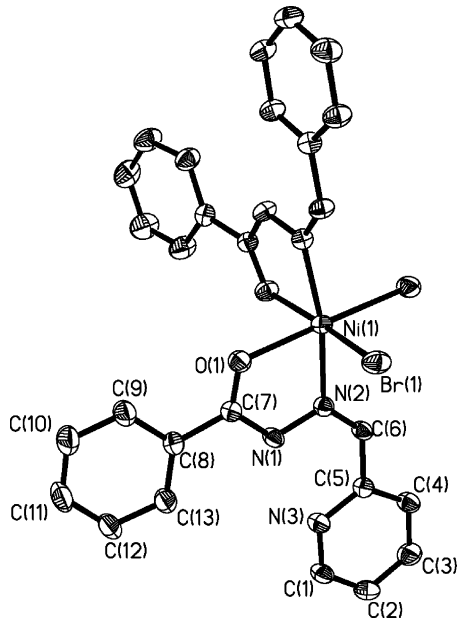

Fig. 4. Molecular structure of **14**, showing 30% probability displacement ellipsoids with hydrogen atoms and molecules of CH_2Cl_2 omitted for clarity.

11 and **15**/MAO system, and it was considered that methyl substituents in the *ortho* position hindered the insertion of norbornene. In entries 4, 7, 10, 13, 19, 22 and 25, monomer can be fully converted into polymer within 30 min. However, complexes **14**–**18**/MAO needed a higher Al/Ni molar ratio to convert norbornene to polymer quantitatively in 30 min, which demonstrate that the pyridyl ligands (**5**–**9**) lowered activity for the catalytic activity of its complex. In addition, polynorbornenes produced by complexes **14**–**18** exhibited lower molecular weight than those generated by complexes **10**–**13** containing diazafluorene analogues. Similarly to our previous results [15], all PNBs produced here are soluble in chlorobenzene. Their IR spectra show no traces of double bonds remaining in the polymer.

To systematically investigate the effects of reaction parameters on vinyl-polymerization of norbornene, the system of diaquabis-[4,5-diazafluorene-9-one-benzoylhydrazone]nickel (**10**) was investigated by changing the reaction parameters such as the solvent, Al/Ni ratio, reaction time, temperature and norbornene/catalyst ratio (norbornene/Ni). The results such as polymer yield, catalytic activity as well as the molecular weight are listed in Tables 4–7, separately, along with the reaction parameters.

The MAO amount is essential for the polymerization of norbornene. Variation of the molar ratio of MAO:nickel complex (Al/Ni) showed considerable effects on polymer yield in either CH_2Cl_2 or toluene (Table 4). The catalytic activity increased with the increase in the Al/Ni molar ratio when it was varied from 100/1 to 500/1, while it decreased with further increasing Al/Ni ratio. At the same time, the molecular weight increased from 580 to 2080 kg/mol when the Al/Ni molar ratio changed from 50 to 75 and decreased to 1290 kg/mol at an Al/Ni molar ratio of 2000. The catalytic activities were in the range of 1.60×10^4 to 9.42×10^5 g PNB/(mol Ni h), and the molecular weight ranged from 580 to 2080 kg/mol. The catalytic activities in toluene were lower than in CH_2Cl_2, and the molecular weight of PNB exhibited a similar tendency.

Table 3
Catalytic behavior of complexes **10**–**18** for the norbornene polymerization

Entry	Complex	Al/Ni	Yield (%)	Activity ($\times 10^5$ g PNB/(mol Ni h))	$\bar{M}_v$ ($\times 10^4$ g/mol)
1	**10**	75	75.5	7.11	208
2	**11**	75	15.1	1.42	58
3	**11**	100	79.8	7.51	192
4	**11**	200	98.5	9.27	176
5	**12**	75	28.8	2.71	105
6	**12**	100	99.6	9.38	195
7	**12**	200	100	9.42	170
8	**13**	75	26.9	2.53	77
9	**13**	100	99.4	9.36	189
10	**13**	200	100	9.42	172
11	**14**	75	0.51	0.05	40
12	**14**	150	89.2	8.40	48
13	**14**	300	99.4	9.36	66
14	**15**	75	2.34	0.22	39
15	**15**	150	84.2	7.93	53
16	**15**	300	97.5	9.18	71
17	**16**	75	6.04	0.57	37
18	**16**	150	86.6	8.16	55
19	**16**	300	99.4	9.36	70
20	**17**	75	2.29	0.22	40
21	**17**	150	89.2	8.40	53
22	**17**	300	100	9.41	77
23	**18**	75	2.97	0.28	40
24	**18**	150	88.1	8.30	47
25	**18**	300	99.9	9.41	77

Polymerization conditions: 25 °C; reaction time, 30 min; dichloromethane; total volume, 25 ml; catalyst, 8 μmol; norbornene/Ni = 5000.

Table 4
The relationship of Al/Ni ratio, polymer yield and catalytic activity of complex **10**

Entry	Solvent	Al/Ni	Yield (%)	Activity ($\times 10^5$ g PNB/(mol Ni h))	$\bar{M}_v$ ($\times 10^4$ g/mol)
26	CH_2Cl_2	50	1.7	0.16	58
1	CH_2Cl_2	75	75.5	7.11	208
27	CH_2Cl_2	100	100	9.42	162
28	CH_2Cl_2	200	100	9.42	143
29	CH_2Cl_2	300	100	9.42	134
30	CH_2Cl_2	500	100	9.42	136
31	CH_2Cl_2	1000	93.0	8.76	129
32	CH_2Cl_2	2000	72.8	6.85	140
33	Toluene	200	22.5	2.12	58
34	Toluene	350	27.6	2.59	72
35	Toluene	500	34.8	3.28	83
36	Toluene	1000	30.4	2.86	95
37	Toluene	1500	30.2	2.84	105
38	Toluene	2500	28.6	2.69	88

Polymerization conditions: 25 °C; reaction time, 30 min; total volume, 25 ml; entries 1, 26–32: 8 μmol catalyst; entries 33–38: 5 μmol catalyst; norbornene/Ni = 5000.

The norbornene polymerization was conducted at different temperatures. The activities have a wavy relationship with the reaction temperature. In CH_2Cl_2, the increase in temperature from −15 to 25 °C results in the increase in the catalytic activity from 2.17×10^5 to 7.11×10^5 g PNB/(mol Ni h) and molecular weight from 1460 to 2080 kg/mol. However, both the catalytic activity and molecular weight of PNB decreased with increasing temperature. The active species could have low thermal stability in CH_2Cl_2. In the case of toluene as solvent, the catalytic activity and molecular weight of resulting PNB decreased gradually with increasing temperature.

Table 5
Influence of the reaction temperature (T) on catalytic activity of complex **10**

Entry	Solvent	T (°C)	Yield (%)	Activity ($\times 10^5$ g PNB/(mol Ni h))	$\bar{M}_v$ ($\times 10^4$ g/mol)
39	CH_2Cl_2	−15	23.0	2.17	146
40	CH_2Cl_2	5	37.6	3.54	161
1	CH_2Cl_2	25	75.5	7.11	208
41	CH_2Cl_2	35	63.3	5.96	52
42	Toluene	0	34.8	3.28	130
35	Toluene	25	34.8	3.28	83
43	Toluene	50	18.9	1.78	28
44	Toluene	75	15.6	1.47	17
45	Toluene	100	10.3	0.97	7

Polymerization conditions: total volume, 25 ml; reaction time, 30 min; norbornene/Ni = 5000; entries 1, 39–41: 8 μmol catalyst, Al/Ni = 75; entries 35, 42–45: 5 μmol catalyst, Al/Ni = 500.

Increase in the monomer concentration (reaction volume and catalyst amount were kept constant), which serve as the increase in the norbornene/Ni ratio, caused rapid increase in catalytic activities combined with a drastic increase in molecular weight. It is easily explained like

Table 6
Influence of the monomer concentration on catalytic activity of complex **10**

Entry	Solvent	Norbornene/Ni	Time (min)	C_M (mol/l)	Yield (%)	Activity ($\times 10^5$ g PNB/(mol Ni h))	$\bar{M}_v$ ($\times 10^4$ g/mol)
46	CH_2Cl_2	1250	30	0.40	39.6	0.93	18
47	CH_2Cl_2	2500	30	0.80	46.6	2.19	23
1	CH_2Cl_2	5000	30	1.60	75.5	7.11	208
48	CH_2Cl_2	10000	30	3.20	43.3	8.15	192
49	CH_2Cl_2	20000	30	6.40	10.3	3.88	118
50	Toluene	2500	30	0.50	17.2	0.81	23
35	Toluene	5000	30	1.00	34.8	3.28	83
51	Toluene	10000	15	2.00	31.6	11.9	137
52	Toluene	15000	10	3.00	23.5	19.9	240
53	Toluene	20000	5	4.00	25.2	56.8	228

Polymerization conditions: 25 °C; total volume, 25 ml; entries 1, 46–49: catalyst, 8 μmol, Al/Ni = 75; entries 35, 50–53: catalyst, 5 μmol, Al/Ni = 500.

Table 7
The relationship of reaction time and catalytic activity of complex **10**

Entry	Solvent	Time (min)	Yield (%)	Activity ($\times 10^5$ g PNB/(mol Ni h))	$\bar{M}_v$ ($\times 10^4$ g/mol)
54	CH_2Cl_2	5	18.0	10.2	171
55	CH_2Cl_2	15	42.2	7.95	177
1	CH_2Cl_2	30	75.5	7.11	208
56	CH_2Cl_2	60	96.2	4.53	176
57	CH_2Cl_2	240	97.5	1.15	171
58	Toluene	5	5.92	3.35	65
59	Toluene	15	13.8	2.60	67
35	Toluene	30	34.8	3.28	83
60	Toluene	60	38.5	1.81	81
61	Toluene	120	54.1	1.27	74
62	Toluene	240	65.6	0.77	73

Polymerization conditions: 25 °C; M/Ni = 5000; total volume, 25 ml; entries 1, 54–57: 8 μmol catalyst, Al/Ni = 75; entries 35, 58–62: 5 μmol catalyst, Al/Ni = 500.

Table 8
Ethylene oligomerization by using **10**–**18**/MAO systems

Entry	Complex	Al/Ni (mol/mol)	Temperature (°C)	Activity ($\times 10^4$ g C_2H_4/(mol Ni h))	Oligomers distribution (%)		
					$C_4/\sum C$	$C_6/\sum C$	Linear α-olefin (C4)
1	**10**	100	30	6.86	98	2	23
2	**10**	500	30	8.56	98	2	41
3	**10**	1000	30	5.65	99	1	45
4	**10**	1500	30	2.30	99	1	43
5	**11**	100	30	5.09	97	3	33
6	**12**	100	30	23.9	83	17	6
7	**13**	50	30	6.08	56	44	99
8	**13**	75	30	10.5	92	8	17
9	**13**	100	30	36.2	76	24	7
10	**13**	200	30	32.6	84	16	11
11	**13**	500	30	6.61	98	2	99
12	**13**	1000	30	4.93	94	6	29
13	**13**	1500	30	4.59	93	7	31
14	**14**	300	30	6.24	100	0	99
15	**14**	500	30	8.28	99	1	28
16	**14**	800	30	10.9	98	2	36
17	**14**	1000	30	9.29	97	3	33
18	**14**	1200	30	7.36	96	4	42
19	**14**	1500	30	3.69	97	3	39
20	**14**	800	0	2.77	88	12	40
21	**14**	800	50	5.04	100	0	1
22	**14**	800	70	3.79	100	0	1
23	**15**	200	30	3.34	100	0	99
24	**15**	1000	30	7.00	96	4	25
25	**15**	1200	30	4.16	96	4	33
26	**16**	200	30	3.80	100	0	99
27	**16**	800	30	6.17	99	1	40
28	**16**	1200	30	3.07	100	0	38
29	**17**	200	30	5.44	100	0	99
30	**17**	500	30	8.38	99	1	50
31	**17**	1200	30	4.84	98	2	43
32	**18**	200	30	6.20	100	0	99
33	**18**	300	30	11.7	100	0	99
34	**18**	1200	30	4.39	99	1	40

Reaction condition: 5 μmol catalyst, 30 ml toluene, 0.5 h, 1 atm ethylene. Using toluene as the internal standard.

the regular olefin polymerization, higher concentration of monomer gives rise to higher catalytic activity and high-order polyolefins. For example in CH_2Cl_2, the catalytic activity was only 9.33×10^4 g PNB/(mol Ni h) at a ratio of norbornene/Ni as 1250:1, whereas the high catalytic activity of 7.11×10^5 g PNB/(mol Ni h) was obtained at a norbornene/Ni ratio of 5000:1 (Table 6), and correspondingly the molecular weight increased from 180 to 2080 kg/mol. In addition, a catalytic activity of 3.88×10^5 g PNB/(mol Ni h) and a molecular weight of 1180 kg/mol were obtained at a norbornene/Ni ratio of 20000:1. Similarly, the catalytic activity and the molecular weight of PNB increased in toluene as solvent when the norbornene/Ni ratio was increased.

The longer the reaction time, the higher the yield of polymer. The results of norbornene polymerization with different time are presented in Table 7. In CH_2Cl_2, the catalytic activity increased rapidly at the beginning of 5–30 min, then increased slightly and leveled off due to a significant decrease in the monomer concentration in the reaction mixture. The conversion of norbornene into PNB was almost complete at 240 min. The molecular weight of PNB reached a maximum at 30 min. Similarly, the polymerization activity, yields and molecular weight changed in toluene with increasing reaction time.

All the polymers obtained have been characterized by IR spectra. The IR spectra prove the absence of a double bond, as no peaks appeared between 1620 and 1680 cm^{-1}. This further ensures the occurrence of vinyl-type polymerization rather than ring-opening metathesis polymerization (ROMP) [24]. ^{1}H NMR (*o*-dichlorobenzene-d_4), δ (ppm): 0.87–2.28 (m, maxima at 0.87, 1.24, 1.59, 2.22). TGA showed that all of the polymer samples were very stable with mass loss of 5–7% up to 450 °C in nitrogen and 350 °C in the air. The determination of the glass transition temperature (T_g) of vinyl homo-polynorbornene is found to be difficult, since it is close to the temperature where decomposition sets in [25]. Our endeavor for the determination of T_g of the obtained vinyl polymers also failed. All the polymer samples obtained were soluble in chlorobenzene at room temperature. No indication

of stereoregularity was observed, which was verified by the amorphous morphology of the products. The resulting polynorbornenes gave similar IR spectra, suggesting their similar unique properties.

4.4. Ethylene oligomerization

4.4.1. Catalytic activity and oligomers distribution

The influence of MAO on catalytic activities and the distribution of resulting oligomers of **10**–**18** were carefully investigated, and the results are summarized in Table 8.

Most complexes showed fairly good activities at the Al/Ni molar ratio of 50–1000. Complex **13** showed the highest catalytic activity of 3.62×10^5 g mol^{-1} atm^{-1} h^{-1} at the Al/Ni molar ratio of 100 at 30 °C. Reaction temperature exerted great influence on catalytic activities of **10**–**18**. Optimal catalytic activities were observed between 0 and 70 °C. The oligomerization products by **10**–**18** were mainly C4 and C6. Compared to the activity [1.23×10^5 g mol^{-1} h^{-1}, Al/Ni = 500] of our previous nickel complexes containing ligand **1**, in which the ligand coordinated with nickel in the keto form [16], the complex **10** with enolate coordination of nickel with ligand **1** showed a lower activity [8.56×10^4 g mol^{-1} h^{-1}, Al/Ni = 500]. The coordination model affected the coordination and insertion of ethylene.

The variation of ligands clearly affected the activities of the corresponding complexes; i.e., the phenyl ring containing an additional alkyl substituent impaired the catalytic activity for ethylene oligomerization. Under the mild catalytic conditions (Al/Ni = 100, 30 °C), **13** with 4-methyl group on the phenyl ring showed a catalytic activity of 3.62×10^5 g mol^{-1} h^{-1}, while **11** with 2-methyl groups on the phenyl ring showed a relatively lower value of 5.09×10^4 g mol^{-1} h^{-1}. As to **14**–**18**, the introduction of chloro and methyl-groups into the ligands affected the catalytic activities. The orders of the activity were **18** > **14** > **17** > **15** > **16**. From the two series of catalytic systems, it is concluded that the **13**/MAO and 18/MAO systems, which contain a methyl substituent in the 4-position of the ligand phenyl ring, show the highest catalytic activities.

5. Conclusions

Complexes **10**–**18** serve as highly active catalysts for the vinyl polymerization of norbornene and reasonable catalysts for oligomerization of ethylene with MAO as cocatalyst. The investigation using complex **10** shows that PNB productivity and molecular weight rely greatly on the ratio of nickel precursor to the amount of MAO and monomer norbornene, as well as the reaction temperature. All PNBs are soluble in chlorobenzene at room temperature and showed similar IR and H NMR spectra. Their catalytic activities, polymer yields, molecular weights and distribution can be controlled by variation of the reaction parameters.

Acknowledgements

We are grateful to the National Natural Science Foundation of China for the sanction of the research grant (No. 20272062). We thank Prof. T. Tatsumi for his kindly English corrections.

Appendix A. Supplementary data

Supplementary data associated with this article can be found, in the online version, at doi:10.1016/j.molcata.2005.01.009.

References

[1] B.L. Goodall, in: B. Rieger, L.S. Baugh, S. Kacker, S. Striegler (Eds.), Late Transition Metal Polymerization Catalysis, Wiley/VCH, Weinheim, 2003.
[2] G.F. Sartori, F. Ciampelli, N. Cameli, Chim. Ind. 45 (1963) 1478.
[3] B.L. Goodall, L.H. McIntosh III, L.F. Rhodes, Macromol. Symp. 89 (1995) 421.
[4] B. Berchtold, V. Lozan, P.-G. Lassahn, C. Janiak, J. Polym. Sci. A 40 (2002) 3604.
[5] S. Rush, A. Reinmuth, W. Risse, Macromolecules 30 (1997) 7375.
[6] T.J. Deming, B.M. Novak, Macromolecules 26 (1993) 7089.
[7] X. Li, Y.-S. Li, J. Polym. Sci. A 40 (2002) 2680.
[8] Y.-Z. Zhu, J.-Y. Liu, Y.-S. Li, Y.-J. Tong, J. Organomet. Chem. 689 (2004) 1295.
[9] (a) W. Keim, Angew. Chem. Int. Ed. Engl. 121 (1990) 235;
(b) W. Keim, F.H. Kowaldt, R. Goddard, C. Krüger, Angew. Chem. Int. Ed. Engl. 17 (1978) 466.
[10] (a) G.J.P. Britovsek, V.C. Gibson, D.F. Wass, Angew. Chem. Int. Ed. Engl. 38 (1999) 428;
(b) S.D. Ittel, L.K. Johnson, M. Brookhart, Chem. Rev. 100 (2000) 1169;
(c) V.C. Gibson, S.K. Spitzmesser, Chem. Rev. 103 (2003) 283;
(d) F. Speiser, P. Braunstein, R. Welter, Organometallics 23 (2004) 2613, 2625, 2633;
(e) W. Zhao, Y. Qian, J. Huang, J. Duan, J. Organomet. Chem. 689 (2004) 2614.
[11] Z. Li, W.-H. Sun, Z. Ma, Y. Hu, C. Shao, Chin. Chem. Lett. 12 (2001) 691.
[12] L. Wang, W.-H. Sun, L. Han, Z. Li, Y. Hu, C. He, C. Yan, J. Organomet. Chem. 650 (2002) 59.
[13] W.-H. Sun, Z. Li, H. Hu, B. Wu, H. Yang, N. Zhu, X. Leng, H. Wang, New J. Chem. 26 (2002) 1474.
[14] H. Yang, Z. Li, W.-H. Sun, J. Mol. Catal. A 206 (2003) 23.
[15] (a) W.-H. Sun, H. Yang, Z. Li, Y. Li, Organometallics 22 (2003) 3678;
(b) H. Yang, W.-H. Sun, F. Chang, Y. Li, Appl. Catal. A 252 (2003) 261;
(c) F. Chang, D. Zhang, G. Xu, H. Yang, J. Li, H. Song, W.-H. Sun, J. Organomet. Chem. 689 (2004) 936.
[16] L. Chen, J. Hou, W.-H. Sun, Appl. Catal. A 246 (2003) 11.
[17] L.J. Henderson Jr., J.F.R. Fronczek, W.R. Cherry, J. Am. Chem. Soc. 106 (1984) 5876.
[18] H.C. Beyerman, J.S. Bontekoe, W.J. Vander Burg, Rev. Trav. Chim. Pas-Bas Belg. 73 (1954) 109.
[19] W. Xiao, Z.L. Lu, B.S. Kang, J. Mol. Struct. 553 (2000) 91.

[20] G.M. Sheldrick, SHELXTL-97, Program for the Refinement of Crystal Structures, University of Gottingen, Germany, 1997.
[21] Z.L. Lu, W. Xiao, Z.N. Chen, X.Y. Gong, S.S.S. Raj, I.A. Razak, H.K. Fun, Acta Crystallogr. C 56 (2000) 1017.
[22] Z.H. Liu, C.Y. Duan, J. Hu, X.Z. You, Inorg. Chem. 38 (1999) 1719.
[23] C. Mast, M. Krieger, K. Dehnicke, A. Greiner, Macromol. Rapid Commun. 20 (1999) 232.
[24] T.F.A. Haselwander, W. Heitz, S.A. Krügel, J.H. Wendorff, Macromolecules 30 (1997) 5345.
[25] P.-G. Lassahn, C. Janiak, J.-S. Oh, Macromol. Rapid Commun. 23 (2002) 16.